

Moisture sources and transport control year-round variations of stable isotopes in precipitation over Bangladesh

Mohammad Rubaiat Islam^{1,3}, Jing Gao^{1,2,*}, Nasir Ahmed⁴, Mohammad Masud Karim⁴,
Abdul Quaiyum Bhuiyan⁴, Shamsuddin Ahmed⁵

¹ Key Laboratory of Tibetan Environment Changes and Land Surface Processes, Institute of Tibetan Plateau Research, Chinese Academy of Sciences, Beijing 100101, China

² CAS Center for Excellence in Tibetan Plateau Earth Sciences, Beijing 100101, China

³ University of Chinese Academy of Sciences, Beijing, 100049, China

⁴ Institute of Nuclear Science & Technology, Bangladesh Atomic Energy Commission, Dhaka, 1207, Bangladesh

⁵ Bangladesh Meteorological Department, Meteorological Complex, Agargaon, Dhaka, 1207, Bangladesh

* Corresponding to: Jing Gao, E-mail: gaojing@itpcas.ac.cn

Abstract

Indian summer monsoon (ISM) has profound impact on water resources over the Asian Water Towers (AWTs) and surroundings. Stable isotopes in precipitation ($\delta^{18}\text{O}$ and δD) are crucial tracers of ISM moisture transport processes. Here we presented spatiotemporal variations of stable isotopes in precipitation at three stations over Bangladesh in 2017-2018 to evaluate the influence of moisture sources and transport on intra-seasonal variations of stable isotopes in precipitation, combined with local meteorological data, ERA5 reanalysis data and HYSPLIT model. We found Bay of Bengal (BoB), tropical Indian Ocean (TIO) and Arabian Sea (AS) were the primary moisture suppliers throughout the year and moisture uptake process primarily occurred over BoB. The most enriched $\delta^{18}\text{O}$ and δD values exist in the pre-monsoon season, associated with >50% contributions from BoB, and gradually decline throughout the monsoon and post-monsoon seasons due to increased contribution of moisture from AS (~30%) and IO (~40%), and reach to their lowest values by the end of the post-monsoon season when >25% contributed from BoB and ~20% from TIO. The strongly positive $\delta^{18}\text{O}$ -OLR and negative $\delta^{18}\text{O}$ -humidity relationships were found at all three stations showing a decreasing pattern from south to north. $\delta^{18}\text{O}$ -temperature ($\delta^{18}\text{O}$ -precipitation) relationship was only found at southern stations at local scale. Convective activities over the AS, BoB and northern IO primarily regulate the $\delta^{18}\text{O}$ depletion, and a weak (strong) flux- $\delta^{18}\text{O}$ relationship for northward (eastward) transport was found. This study could improve understanding of moisture transport by the ISM for our societies to promote the water resource management over AWTs.

37 *Keywords: Indian summer monsoon, deuterium excess, convective activity, meteorological*
38 *influence, moisture transport*

39 **1. Introduction**

40 The Indian summer monsoon (ISM) is directly associated with water resources and
41 hydroclimate-related natural disasters in the Asian Water Towers (AWTs), influencing the
42 lives and livelihoods of more than 2 billion people. Understanding the contribution of
43 moisture transported by the ISM is crucial for the projection of the regional water cycle and
44 evaluation of the water supply from AWTs to surrounding regions [Breitenbach *et al.*, 2010;
45 Cai *et al.*, 2018; Mukherjee *et al.*, 2007]. Instrumental records of traditional meteorological
46 parameters have already provided plenty of information to understand the dynamics of the
47 ISM [Ahmed and Karmakar, 1993; Ananthakrishnan and Soman, 1988; Day *et al.*, 2015;
48 Rafiuddin *et al.*, 2010]. However, this information is still not enough to illuminate regional
49 moisture transport processes and quantify the moisture contribution from the Bay of Bengal
50 (BoB) to the AWTs. Water stable isotopes, water molecules consisting of stable isotopes of
51 hydrogen and oxygen, were frequently used to quantify atmospheric water budget, predict
52 moisture source region, and track isotopic fractionation occurred at different reservoirs of the
53 global hydrologic cycle. Due to their efficiency as tracers of water transfer, water stable
54 isotopes can improve our understanding on the variation of ISM throughout Earth's
55 evolutionary history [Cai and Tian, 2016; Chakraborty *et al.*, 2016; Rahul *et al.*, 2016; Yang
56 *et al.*, 2016]. ISM-driven moisture from the BoB is transported to the AWTs through
57 Bangladesh (extending from 20°34'N to 26°38'N latitude and 88°01'E to 92°41'E longitude,
58 Figure 1). Therefore, the event-based observations of stable isotopes in precipitation provide
59 a unique tool to evaluate the contribution of different moisture sources and transport to
60 Bangladesh before reaching to AWTs.

61 Isotopes are atoms of the same element that has the same number of protons in their atomic
62 nucleus with a difference in the number of neutrons. Stable isotopes do not spontaneously
63 decay into another isotope or atom and several naturally occurring stable isotopes of oxygen
64 (¹⁶O, ¹⁷O, and ¹⁸O) and hydrogen (¹H and ²H or D) can be found in natural environment. Due
65 to a very small abundance of the heavier isotopes compared to that of the lighter one, the
66 concentration of the heavier isotopes is often expressed as isotopic ratios. Isotopic ratios of
67 ¹⁸O and D can be expressed using δ notation as $\delta^{18}\text{O}$ and δD . Based on isotopic

68 measurements of meteoric water samples from different parts of the world, *Craig* [1961]
69 established a linear relationship between δD and $\delta^{18}O$:

$$70 \quad \delta D = 8 * \delta^{18}O + 10$$

71 This relationship is commonly referred to as the global meteoric water line (GMWL). The
72 GMWL serves as a good indicator of post sampling evaporation because samples that did not
73 undergo excessive evaporation will display a strong linear correlation between δD and $\delta^{18}O$.
74 In studying regional and local hydrological processes, the local meteoric water line (LMWL)
75 is used to express the relationship between δD and $\delta^{18}O$ in a region. *Putman et al.* [2019]
76 investigated the global distribution of LMWLs and suggested that the δD - $\delta^{18}O$ relationship in
77 the LMWL stems from the interplay of water isotope systematics and hydroclimatic
78 seasonality at a given site. Relative differences in geographical location also lead to subtle
79 variations in the slope and intercept of the LMWL [*Putman et al.*, 2019]. Therefore,
80 differences in the slope and intercept between the LMWL and GMWL can be used to trace
81 moisture sources and estimate the degree of sub cloud evaporation [*Putman et al.*, 2019;
82 *Wang et al.*, 2019].

83 Many previous studies documented the effects of local meteorological variations and
84 atmosphere circulations as well as convective activities on precipitation stable isotopes
85 worldwide. *Dansgaard* [1964] established the ‘temperature effect’ (decrease in δ -values with
86 increasing temperature) and ‘amount effect’ (higher δ -values in sparse rain) as two of the
87 important mechanisms controlling stable isotopic variation in precipitation. The amount
88 effect is primarily noticeable in low-latitude regions that are influenced by monsoons, while
89 the influence of the temperature effect is significant in temperate and polar regions [*Zhang et*
90 *al.*, 2019]. However, the majority of recent studies over the Indian subcontinent suggested
91 that the amount effect is weak and even nonexistent in this region [*Araguas-Araguas et al.*,
92 1998; *Bhattacharya et al.*, 2003; *Breitenbach et al.*, 2010; *Datta et al.*, 1991; *Midhun et al.*,
93 2013; *Tang et al.*, 2015].

94 Investigations of the influences of convective activities and moisture transport processes on
95 precipitation stable isotopes have grown in the past 20 years. *Bhattacharya et al.* [2003]
96 revealed that precipitation stable isotopes at Bombay and New Delhi bear a greater influence
97 to the moisture source region and that lower (higher) $\delta^{18}O$ values were associated with
98 oceanic (continentally recycled) moisture sources. *Breitenbach et al.* [2010] studied air parcel

99 travel distance histories during parcel transport from vapor source regions and found that
100 lower (higher) $\delta^{18}\text{O}$ values were associated with long (short) transport distances at Southern
101 Meghalaya, NE India. *Lekshmy et al.* [2015] and *Chakraborty et al.* [2016] studied the
102 convective influence on $\delta^{18}\text{O}$ and found that lower $\delta^{18}\text{O}$ values occur when air parcels come
103 across a convective system over the Indian Ocean. *Midhun et al.* [2018] investigated moisture
104 transport pathways and found that $\delta^{18}\text{O}$ -depleted (enriched) precipitation events were
105 associated with a higher number of air parcel trajectories originating from the Bay of Bengal
106 (Arabian Sea) branch of moisture transport at six stations across northern and central India.
107 By investigating isotopic relationship between the source moisture, ambient vapor and
108 rainwater, *Sinha and Chakraborty* [2020] suggested that isotopic composition in precipitation
109 over Port Blair, BoB is influenced by the interaction of precipitation with source and ambient
110 vapor. Event scale $\delta^{18}\text{O}$ values in precipitation and ambient vapor displayed significant
111 correlation over a wide range of rainfall amount, however, correlation considerably weakened
112 for rainfall exceeding ~ 36 mm/day. Weaker correlation during heavy rainfall events might
113 have resulted from the limitations of the Rayleigh fractionation and Craig-Gordon Model.
114 Therefore, isotopic variability in source moisture should be considered for the comprehensive
115 isotopic studies over the coastal regions. Their case study suggested that vapor-rainwater
116 isotopic exchange contributes to $\delta^{18}\text{O}$ enrichment in subsequent precipitation events. *Tanoue*
117 *et al.* [2018] reported seasonal variation of stable isotopes in precipitation and the influence
118 of moisture source variation over Bangladesh during January to December 2010. Based on
119 IsoGSM simulations they suggested that moisture from the BoB and Arabian Sea (AS)
120 primarily contributed to pre-monsoon precipitation, while, the influence from the BoB and
121 AS decreased significantly in ISM season when moisture predominantly originated from the
122 Indian Ocean (IO). In post-monsoon season, moisture from Pacific Ocean (PO), BoB and
123 continentally recycled moisture primarily contributed to precipitation over Bangladesh.
124 *Tanoue et al.* [2018] provided an improved understanding on moisture source variation,
125 however, understanding on local and regional meteorological influence is still limited.
126 Moreover, their studies comprising of three stations primarily focused on eastern and central
127 part. however, understanding of isotopic variation over southern part of Bangladesh where
128 ISM moisture makes the first interaction with land is poorly understood.

129 To improve our understanding of the relationship between moisture sources and stable
130 isotopic compositions of precipitation over Bangladesh, the current study presented the event-
131 based precipitation stable isotopes during February 2017 and September 2018. In section 2,

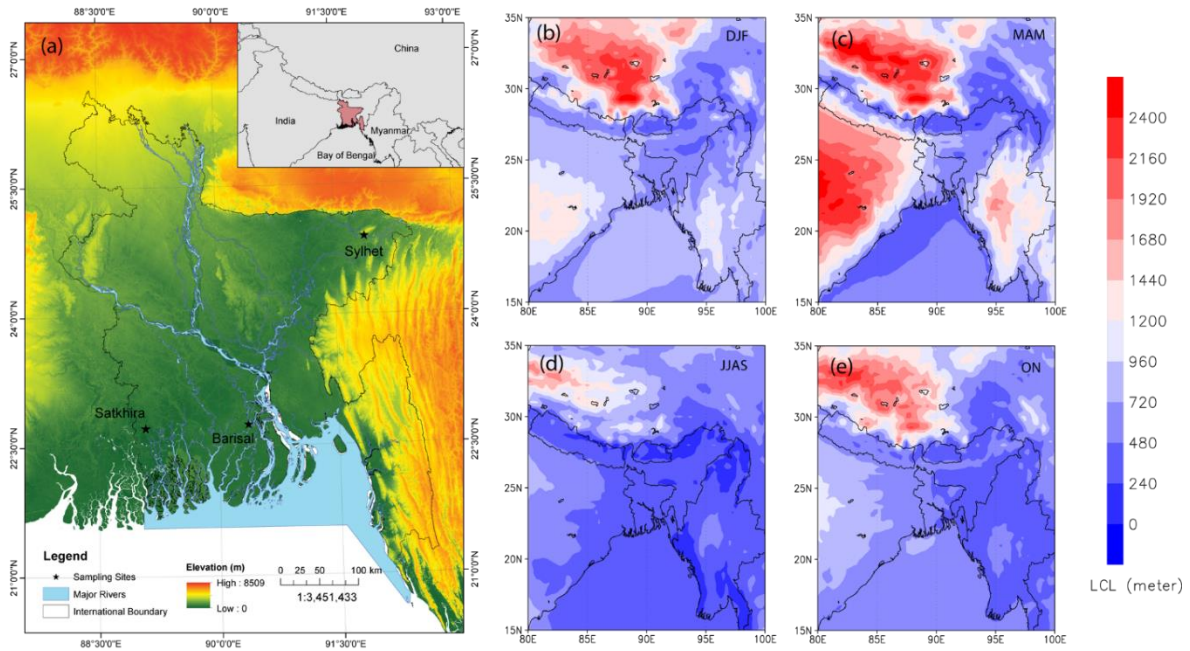
132 we provide details of study area and data used in this study. In section 3, we probe the local
133 meteorological influence by correlation analysis between event-based precipitation $\delta^{18}\text{O}$ and
134 meteorological observations (air temperature, precipitation amount and relative humidity) and
135 regional moisture influence by combined analyses with back trajectory, outgoing longwave
136 radiation (OLR) and regional meteorological elements. Conclusions and perspectives are
137 provided in the last section. This study improved our understanding of the ISM influence on
138 precipitation stable isotopes and could help us to understand behavior of ISM moisture,
139 which is necessary for our societies to address hydroclimatic disasters and promote water
140 resource management over AWTs.

141

142 **2. Materials and Methods**

143 **2.1 Study Area**

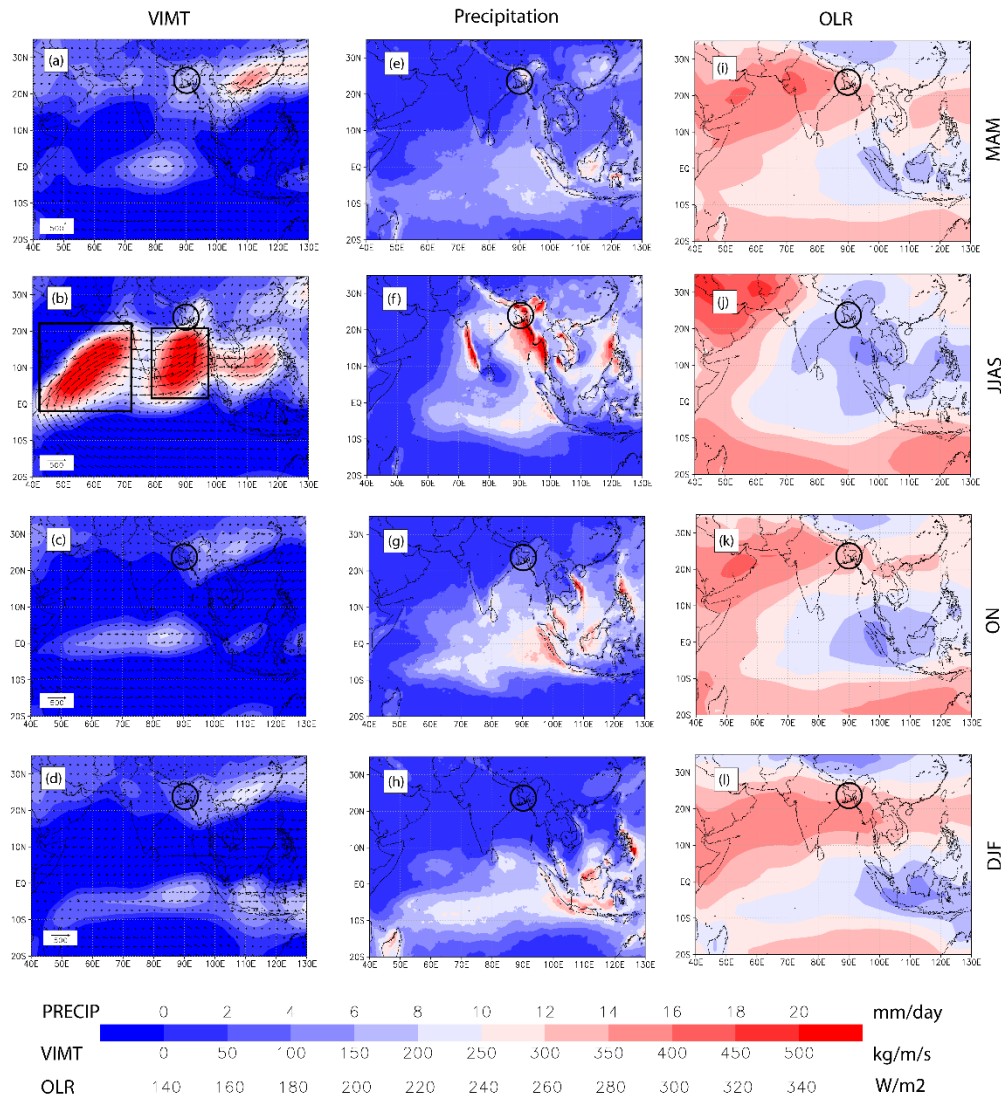
144 Located in the tropical monsoon region, Bangladesh is in the south of Himalayas and is
145 southwardly open to the BoB (extending from 20°34'N to 26°38'N latitude and 88°01'E to
146 92°41'E longitude, Figure 1) where ISM-driven moisture first interact with land on its way to
147 AWTs. The climate of Bangladesh is characterized by moderately warm temperatures and
148 high relative humidity with marked seasonal variations in rainfall related to ISM [*Pour et al.*,
149 2018]. Four seasons distinguish the climate of Bangladesh, namely, pre-monsoon (March-
150 May), monsoon (June-September), post-monsoon (October-November) and winter
151 (December-February) [*Dewan et al.*, 2018; *Fahad et al.*, 2018; *Pour et al.*, 2018; *Whitehead*
152 *et al.*, 2018].



153

154 Figure 1: Location of precipitation sample collection sites (a) and 1979-2018 average
 155 seasonal lifting condensation level (LCL) climatology over the study area (b-e).

156 The pre-monsoon (MAM) period is characterized by the highest evapotranspiration rate and
 157 temperature with the occurrence of occasional line squalls and tropical cyclones in coastal
 158 areas. Nineteen percent of the total annual rainfall occurs in MAM, and the average air
 159 temperature ranges between 23.50°C and 30.30°C. Moisture mainly comes from the
 160 Mediterranean region, which occasionally contributes to heavy rainfall that causes flooding
 161 [Rimi *et al.*, 2019]. In JJAS, more than 70% of the total annual rainfall occurs with the
 162 highest cloudiness [Das, 2017; Mullick *et al.*, 2019], and the temperature ranges between
 163 27.40°C and 29.80°C. a tremendous amount of moisture is transported through Bangladesh to
 164 the AWTs. In The post-monsoon (ON), 8% of the total annual rainfall occurs, and the
 165 temperature ranges between 22.20°C and 27.90°C. Only 2% of the total annual rainfall
 166 occurs in the winter DJF, and the temperature ranges are between 16.30°C and 23.30°C. In
 167 this study, we primarily focused on MAM, JJAS and ON, and exclude DJF because of the
 168 very small number of precipitation events in that season.



169

170 Figure 2: The 2015-2019 average vertically integrated moisture transport (a-d) illustrates the
 171 regional moisture transport (in vectors) and moisture flux (shaded color) in the region during
 172 different seasons. Additionally, the 1998-2018 average seasonal precipitation (e-h) and OLR
 173 (i-l) distribution in the region are included. Two rectangles indicate regions where maximum
 174 total flux centered in JJAS, while, the circle indicates location of Bangladesh.

175 Figure 2 illustrates the spatial distribution of seasonal average precipitation, OLR and
 176 moisture transport in the region. As discussed earlier, maximum precipitation (~3000 mm)
 177 occurs in JJAS over the northeastern part of Bangladesh, the western part of Myanmar and
 178 the southwestern part of India. The seasonal average precipitation in these regions was ~20
 179 mm/day. Although the southwestern part of India received more rainfall in JJAS, it was
 180 relatively small over the southeastern part. In MAM, higher (~10 mm/day) rainfall occurred

181 over the northeastern part of Bangladesh and the southern part of Myanmar, Thailand and
182 Indonesia. Although Bangladesh received little rainfall in ON, it was significantly higher over
183 Indonesia, Vietnam and Thailand. In DJF, precipitation occurred only over Indonesia but
184 seasonal average precipitation amount was small (<10 mm/day). Seasonal average OLR for
185 MAM displayed higher values at majority of places in the region indicating significant
186 reduction in convective activities. Lower values were only observed in Indonesia (~ 200 - 220
187 W/m^2), while, it was ~ 320 W/m^2 over western part of India. OLR over Bangladesh typically
188 ranged in between 260 - 300 W/m^2 . In JJAS, OLR decreased significantly over ISM regions,
189 particularly, BoB, eastern part of India, Bangladesh, Myanmar and Thailand. Seasonal
190 average OLR remained within 200 - 240 W/m^2 range over the ISM region, while, higher
191 values were observed over Pakistan, Afghanistan and Mediterranean regions (280 - 320
192 W/m^2). In ON, lowest OLR values were observed over Indonesia with significantly higher
193 values over the north-western part of India, while, significantly higher (~ 300 W/m^2) values
194 were observed for DJF within 10 - 20°N latitude band. We also found a distinct pattern for
195 vertically integrated moisture transport (VIMT) in the region. The total moisture flux (sum of
196 zonal and meridional flux) was ~ 100 kg/m/s during MAM and ON; however, it increased
197 significantly to ~ 500 kg/m/s in JJAS due to the development of ISM. The maximum total flux
198 was centered over AS adjacent to India and the BoB (Figure 2).

199 **2.2 Sampling and Laboratory Analysis**

200 Event-based precipitation samples were collected at the Barisal, Satkhira and Sylhet stations
201 located in the southwestern, southcentral and northeastern parts of Bangladesh (Figure 1).
202 Basic information about these sampling stations can be found in Table 1. From February
203 2017 to September 2018, a total of 502 event-based precipitation samples were collected at
204 the Barisal, Satkhira and Sylhet stations with assistance from the Bangladesh Atomic Energy
205 Commission (BAEC). During our sampling period, the air temperature remained within the
206 12.8 - 34°C range with an average of $\sim 25^\circ\text{C}$. Approximately 70% of the total annual rainfall
207 occurred in JJAS, and therefore, we consider our study period a representative sample for a
208 typical monsoon year representing an identical stable isotopic composition in precipitation.
209 All these stations are manned to ensure continuous operations, and each precipitation event
210 yielded only one sample bottle, which was filled as much as possible. The humid
211 environment, immediate collection and cold storage facilities ensured minimal post-sampling
212 evaporation. Samples were later transported to the Key Laboratory of Tibetan Plateau

213 Climate Change and Land Surface Processes, Chinese Academy of Sciences for laboratory
214 analysis.

215 Table 1: Geographic information and 1980-2010 average seasonal precipitation amounts

Station	Number of Samples	Geography			Precipitation (mm)			
		Lat (N)	Lon (E)	Elev (m)	DJF	MAM	JJAS	ON
Barisal	130	22.75	90.36667	10	48.5	422.3	1446.4	211.0
Satkhira	114	22.71667	89.08333	10	65.2	276.5	1249.4	151.8
Sylhet	258	24.9	91.883333	20	55.0	1100.5	2786.2	254.3

216 Measurements were performed with a Picarro Li-2130 analyzer using a cavity ring-down
217 system at an analysis rate of 18-21 samples per batch, not including standard samples.
218 Analytical uncertainties for $\delta^{18}\text{O}$ and δD were $\pm 0.1\%$ and $\pm 0.4\%$, respectively. One primary
219 (USGS50) and one secondary standard of identical isotopic compositions with respect to
220 sample values were used during measurements, with the secondary standard being the main
221 standard. All the precipitation and standard samples were continuously injected six times. To
222 avoid the memory effect of the analyzer during isotopic measurements, the first three
223 injections were discarded, and the average of the last three injections was used in the
224 analyses. All the standard samples were tested against Vienna Standard Mean Ocean Water
225 (VSMOW) and were selected based on our empirical knowledge of the isotopic composition
226 of measured samples in the region.

227 **2.3 Meteorological Data**

228 The daily air temperature, relative humidity and precipitation amount data collected from the
229 Bangladesh Meteorological Department (BMD) are used in this study to detect the local
230 meteorological influence. The daily air temperature and relative humidity data at the 1000
231 hPa level from the European Centre for Medium-Range Weather Forecasts (ECMWF) ERA5
232 reanalysis as well as precipitation data from the Tropical Rainfall Measurement Mission
233 (TRMM) are used for regional analysis. Multisatellite estimates from the TRMM daily
234 precipitation product (3B42 V7.0) come with gauge calibration and were selected because of
235 their higher spatial resolution ($0.25^\circ \times 0.25^\circ$) and extensive usage in previous studies

236 [Chakraborty *et al.*, 2016; Rahul and Ghosh, 2019; Rohrmann *et al.*, 2014; Vimeux *et al.*,
237 2005]. To evaluate the influence of convective activities on precipitation $\delta^{18}\text{O}$, we used OLR
238 data from NOAA's National Centers for Environmental Information (NCEI) website
239 available at <https://www.ncei.noaa.gov/data/outgoing-longwave-radiation-daily/access/>.

240 **2.4 Lagrangian Back Trajectory Analysis and Moisture Fluxes**

241 Using the Hybrid Single-Particle Lagrangian Integrated Trajectory model (HYSPLIT)
242 developed at the Air Resources Laboratory of National Oceanic and Atmospheric
243 Administration (NOAA), we performed back trajectory analysis to identify moisture sources
244 and transport pathways [Stein *et al.*, 2015]. The September 2019 release (version 4.2.0) of
245 HYSPLIT was used in this study. Meteorological data from the Global Data Assimilation
246 System (GDAS) were used for the computation of daily trajectory endpoints because of their
247 higher spatial resolution ($1.0^\circ \times 1.0^\circ$) compared with those of the National Centers for
248 Environmental Prediction (NCEP) data ($2.5^\circ \times 2.5^\circ$). A higher spatial resolution enables us to
249 minimize errors in calculating trajectories; therefore, the majority of recent studies used
250 GDAS to perform the HYSPLIT simulations [Kostrova *et al.*, 2020; Munksgaard *et al.*, 2020;
251 Saranya *et al.*, 2018; Sinha *et al.*, 2019; Wu *et al.*, 2019; Zhang *et al.*, 2019].

252 We used 500 m AGL as the starting height because our analysis for the 1979-2018 average
253 LCL suggests that air parcels typically become saturated with moisture at this height over
254 Bangladesh throughout the year (Figure 1). We computed trajectories in reverse mode
255 (backward in time, inverting the wind components) for 120 hours, and at each point, particles
256 were released every 6 hours (at 0000, 0600, 1200, and 1800 UTC). Later, trajectory endpoints
257 for days with precipitation events were used for cluster analyses. Statistical clustering of
258 similar trajectories was performed through HYSPLIT's internal clustering module. Changes
259 in specific humidity along the clustered trajectories were also computed to obtain a clear
260 visualization of the moisture uptake process in the region.

261 **3. Results and Discussion**

262 **3.1 Temporal Variation in Precipitation $\delta^{18}\text{O}$**

277 (Sylhet, -15.88‰ to 4.01‰) and southern (Barisal, -16.12‰ to 1.61‰ and Satkhira, -18.58‰
278 to 2.64‰) parts of Bangladesh were similar. Our observations were consistent with *Tanoue et*
279 *al.* [2018], who reported stable isotopic variation in precipitation over Bangladesh within the
280 -15.0‰ to 1.0‰ range. The average amount weighted deuterium excess values were 6.16‰,
281 10.94‰ and 11.93‰ for the Satkhira, Barisal and Sylhet stations, respectively showing
282 similar decreasing pattern from west to east. At Satkhira station located to the south-western
283 part of Bangladesh displayed the highest $\delta^{18}\text{O}$ and lowest deuterium excess values throughout
284 MAM and JJAS suggesting a stronger influence of sub-cloud evaporation. Although we did
285 not include δD in the figure, the variations in δD were identical to $\delta^{18}\text{O}$ because they are
286 mathematically related to each other.

287

288

289 Table 2: Summary statistics for annual and seasonal amount weighted average $\delta^{18}\text{O}$, δD and
 290 deuterium excess at Barisal, Satkhira and Sylhet Station during 2017-2018 period. Also
 291 included seasonal maximum and minimum $\delta^{18}\text{O}$, δD and deuterium excess values for Barisal,
 292 Satkhira and Sylhet

Time	Statistic	Barisal			Satkhira			Sylhet		
		$\delta^{18}\text{O}$	δD	d-excess	$\delta^{18}\text{O}$	δD	d-excess	$\delta^{18}\text{O}$	δD	d-excess
Annual	Average	-5.40	-34.15	10.94	-4.01	-25.90	6.16	-5.07	-28.62	11.93
DJF	Minimum	-7.80	-50.26	11.81	N/A	N/A	N/A	-13.62	-101.30	2.41
	Maximum	-7.68	-48.83	12.70	N/A	N/A	N/A	-1.17	1.76	13.71
	Average	-7.79	-50.11	12.19	N/A	N/A	N/A	-5.81	-33.87	9.61
MAM	Minimum	-8.75	-60.88	3.78	-2.88	-6.67	-5.52	-10.77	-80.51	0.20
	Maximum	1.12	17.53	16.35	1.73	18.66	16.33	4.01	43.39	20.48
	Average	-1.78	-12.16	11.58	0.88	10.20	3.17	-1.97	-2.51	13.25
JJAS	Minimum	-16.12	-117.44	6.20	-15.91	-114.78	-12.79	-15.88	-113.11	3.36
	Maximum	1.61	19.82	15.96	2.64	20.48	13.63	-0.01	12.48	16.65
	Average	-6.20	-39.28	10.35	-4.22	-26.71	7.05	-6.73	-43.09	10.76
ON	Minimum	-11.90	-83.72	7.13	-18.58	-134.80	8.42	-14.21	-102.95	4.89
	Maximum	-4.36	-24.30	15.37	-4.97	-27.33	13.81	-7.28	-48.12	15.73
	Average	-8.99	-60.31	11.65	-10.82	-76.16	10.37	-8.89	-59.08	12.06

293 Table 2 lists average, minimum and maximum $\delta^{18}\text{O}$, δD and deuterium excess values of
 294 precipitation at different seasons along with annual average at Satkhira, Barisal and Sylhet
 295 stations. Satkhira station did not have any precipitation samples for DJF. Seasonal average
 296 $\delta^{18}\text{O}$ (δD) values for DJF at Barisal and Sylhet station were -7.79‰ (-50.11‰) and -5.81‰ (-
 297 33.87‰). At Barisal and Sylhet station, deuterium excess values for DJF were closely aligned
 298 with 10.0‰ that equal to global mean deuterium excess in precipitation. In DJF, $\delta^{18}\text{O}$ and δD
 299 displayed the most enriched values at the northern station (Sylhet), while, it was significantly
 300 depleted at Barisal. In MAM, average $\delta^{18}\text{O}$ values for Satkhira, Barisal and Sylhet stations
 301 were 0.88‰, -1.78‰ and -1.97‰, respectively showing significant isotopic enrichment at
 302 Satkhira and eastward increase in isotopic depletion. δD showed similar pattern with an
 303 average of 10.20‰, -12.16‰ and -2.51‰, respectively. Average deuterium excess for MAM

304 had the smallest values at Satkhira (3.17‰), although they were considerably higher at
305 Barisal (11.58‰) and Sylhet (13.25‰). In JJAS, average $\delta^{18}\text{O}$ (δD) values at Satkhira,
306 Barisal and Sylhet were -4.22‰ (-26.71‰), -6.20‰ (-39.28‰) and -6.73‰ (-43.09‰),
307 respectively showing eastward decreasing trend. Deuterium excess values were the smallest
308 at Satkhira (7.05‰) although they were significantly higher at Barisal (10.35‰) and Sylhet
309 (10.76‰). In ON, average $\delta^{18}\text{O}$ (δD) values for Satkhira, Barisal and Sylhet stations were -
310 10.82‰ (-76.16‰), -8.99‰ (-60.31‰) and -8.89‰ (-59.08‰) making it the seasons with
311 the most depleted values in the year. $\delta^{18}\text{O}$ and δD values displayed an eastward increasing
312 trend having the most enriched values in the east, In ON, deuterium excess values for all
313 three stations were above 10.0‰ with maximum and minimum values at Sylhet (12.06‰) and
314 Satkhira (10.37‰).

315 At the monthly scale, a decreasing trend in $\delta^{18}\text{O}$ starting in May was found (Figure 3), $\delta^{18}\text{O}$
316 became the lowest (\sim -10.0‰) in October, then the $\delta^{18}\text{O}$ values started to increase again till
317 December (\sim 0.0‰). The monthly average $\delta^{18}\text{O}$ ranged between -12.0‰ and 3.0‰
318 throughout the study period, with March-May $\delta^{18}\text{O}$ values within the -5.0‰ to 3.0‰ range,
319 while the range for July-November was -12.0‰ to -6.0‰. Previously, *Tanoue et al.* [2018]
320 reported March-May $\delta^{18}\text{O}$ values for the eastern part of Bangladesh within the -1.82‰ and -
321 3.45‰ range, while they were between -7.28‰ and -15.94‰ during the July-November
322 period, similar with our observation. Variations in OLR seem to have similar patterns with
323 $\delta^{18}\text{O}$, especially during MAM and JJAS, which show gradual decreases after April from \sim 300
324 W/m^2 to \sim 200 W/m^2 . Temperature correspondingly increase from winter (\sim 20°C) to summer
325 (\sim 30°C) and have an inverse relationship with $\delta^{18}\text{O}$. An inverse relationship between $\delta^{18}\text{O}$
326 and humidity was also found; however, it was difficult to establish a significant relationship
327 between precipitation amount and $\delta^{18}\text{O}$. The monthly average precipitation range at Sylhet
328 (0.0 mm/day to 30.0mm/day) was significantly higher than that of the Barisal and Satkhira
329 stations (0.0 mm/day to 16 mm/day). Monthly amount weighted deuterium excess values in
330 precipitation for Barisal and Sylhet stations were found in between 8.25‰ and 15.73‰
331 range, while, it was significantly depleted for Satkhira ranging from 0.09‰ to 11.11‰.
332 Monthly deuterium excess values at Satkhira station remained below 3.30‰ during March-
333 August 2017, while, it was $>$ 8.25‰ for Barisal and Sylhet throughout the study period.

334 Majority of heavy rainfall ($>$ 50 mm) events occurred in monsoon season when we observed
335 significant isotopic depletion, however, non-monsoon heavy rainfall events deviated this rule

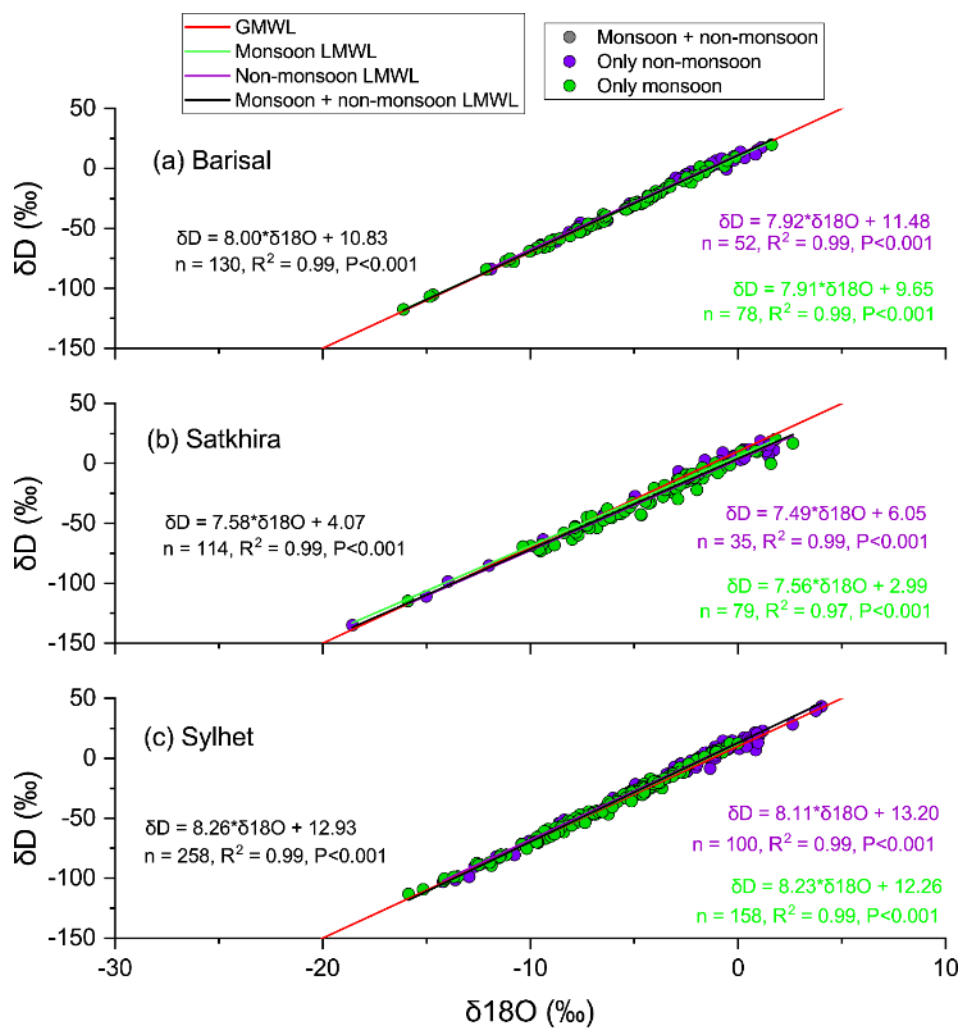
336 significantly. At Sylhet station, we observed several heavy rainfall events in MAM that
337 contributed to flash flood in 2017 [Rimi *et al.*, 2019]. At Sylhet station, >70 mm daily rainfall
338 was recorded for six consecutive days during March 30 and April 4, 2017 however, we found
339 little change in $\delta^{18}\text{O}$ values from pre and post heavy rainfall events. When we compared
340 MAM heavy rainfall events with those that occurred during October 20-22, 2017, we found
341 ON heavy rainfall events resulted in a significant $\delta^{18}\text{O}$ depletion at all three stations. Satkhira
342 station displayed the strongest isotopic depletion where $\delta^{18}\text{O}$ values became as low as -
343 20.0‰. However, we found no $\delta^{18}\text{O}$ depletion during MAM heavy rainfall events. Based on
344 back trajectory analysis and evaluated changes in specific humidity (~15.0 g/kg) along the
345 clustered trajectories, we found that, moisture from BoB accounted for >50% of total air mass
346 trajectories for MAM, while, >20% trajectories for ON originated over AS or tropical Indian
347 Ocean (TIO). *Midhun et al.* [2018] found that $\delta^{18}\text{O}$ -depleted (enriched) precipitation events
348 were associated with a higher number of air parcel trajectories originating from the BoB (AS)
349 branch of moisture transport at six stations across northern and central India. Moreover,
350 moisture from BoB had relatively short transport distance from the source region, while, it
351 was significantly long for AS and TIO. Breitenbach *et al.* [2010] found that lower (higher)
352 $\delta^{18}\text{O}$ values for precipitation at Southern Meghalaya, NE India were associated with long
353 (short) transport distance. Therefore, we conclude that, such a discrepancy in $\delta^{18}\text{O}$ depletion
354 between MAM and ON heavy rainfall events were resulted from source moisture effect and
355 this conclusion is consistent with Breitenbach *et al.* [2010] and *Midhun et al.* [2018].

356 **3.2 Local Meteoric Water Line**

357 We used the ordinary least square regression method to calculate the LMWL from the
358 unweighted event-scale δD and $\delta^{18}\text{O}$ values obtained through isotopic measurements to
359 enable our results to be easily comparable with the published literature on meteoric water
360 lines in this region [*Crawford et al.*, 2014; *Hughes and Crawford*, 2012; *Putman et al.*, 2019].

361 Figure 5 illustrates the δD - $\delta^{18}\text{O}$ relationship observed at different timescales (throughout the
362 study period, only during the monsoon season and only during the non-monsoon season) at
363 the Barisal, Satkhira and Sylhet stations. Among the stations, the highest LMWL slopes were
364 found at Sylhet, while the lowest exist at Satkhira in both the monsoon and non-monsoon
365 seasons, which indicate the significant evaporation occurred at Sylhet (8.23 and 8.11 for
366 monsoon and non-monsoon) and weak condensation at Satkhira (7.56 and 7.49 for monsoon
367 and non-monsoon, respectively). The LMWL slopes were smaller in the non-monsoon season

368 than in the monsoon season, suggesting higher condensation effects in the non-monsoon
 369 season for the Satkhira and Sylhet stations. Slopes at Barisal are very close to GMWL (8 for
 370 annual, 7.91 and 7.92 for monsoon and non-monsoon, respectively). During the 2017-2018
 371 period, the LMWL intercepts displayed an increasing trend from west to east with the
 372 smallest values at Satkhira (4.07), while they were the largest at Sylhet (12.93). Intercepts at
 373 the Barisal were close to the GMWL intercepts (10.83), indicating the wetter moisture
 374 sources in the west than that in the east. The smallest (highest) values in the monsoon (non-
 375 monsoon) season at all three stations due to >80% (~20% in DJF) moisture originating from
 376 oceans.



377

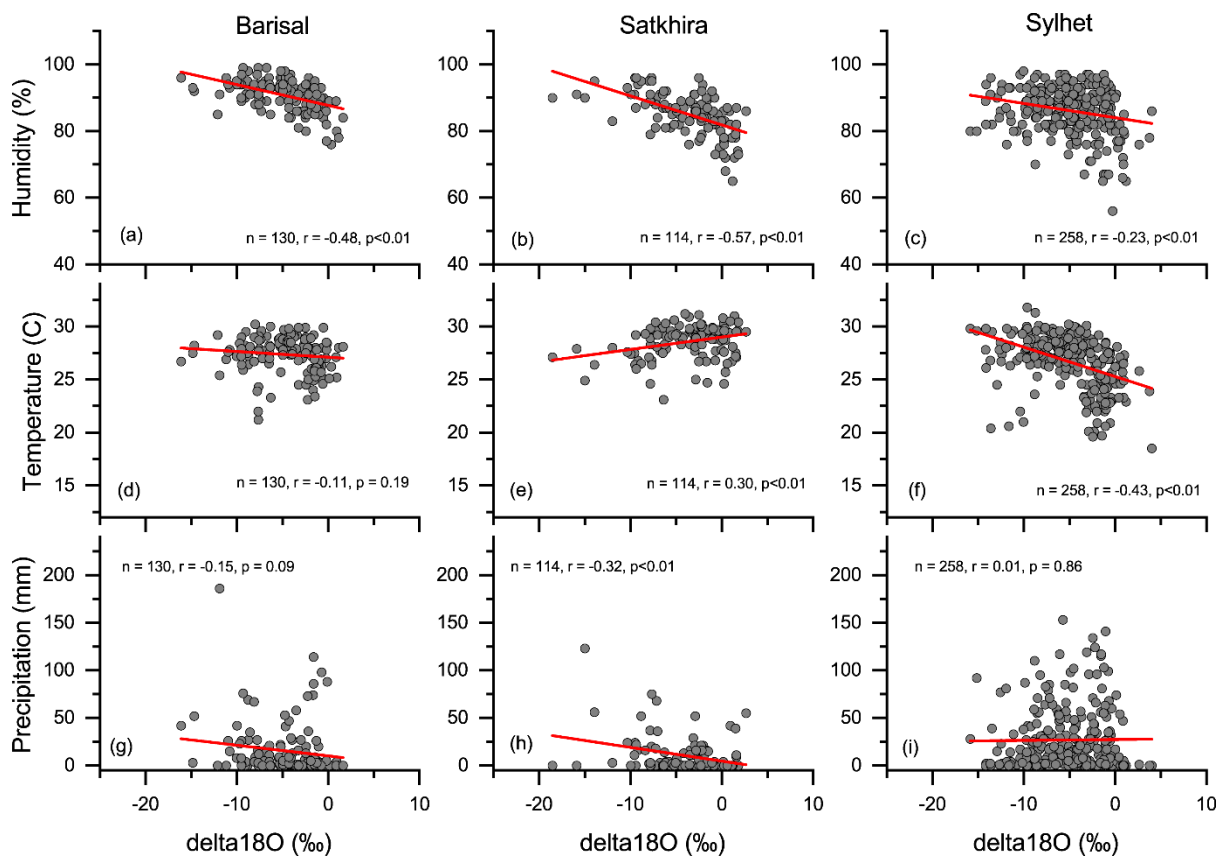
378 Figure 4: LMWL showing the $\delta^{18}O$ - δD relationship and their deviation from the GMWL
 379 proposed by *Craig* [1961]

380 *Jeelani et al.* [2018] studied stable isotopic variation at Jorhat station located near Sylhet,
 381 where we found very close LMWL slopes (8.23 at Sylhet and 8.38 at Jorhat) for the monsoon

382 season; however, a large discrepancy was found for the non-monsoon season slope calculated
 383 at the Sylhet station (8.11) from that reported for the westerly disturbance period (7.70) at the
 384 Jorhat station. This may result from different years' sampling. Previously, *Kumar et al.*
 385 [2010] established the Indian meteoric water line (IMWL) as $\delta D = 7.93 * \delta^{18}O + 9.94$ and
 386 reported 8.15, 7.82 and 7.95 as the slopes for the northern India, southern India and western
 387 Himalayan meteoric water lines, respectively. Although the LMWL slopes for the Sylhet
 388 station (northeastern part of Bangladesh) were consistent with the findings of *Kumar et al.*
 389 [2010], considerable differences were found between the Barisal and Satkhira stations
 390 (southern part of Bangladesh). The LMWL slopes at the Barisal station (8.00) were higher
 391 than those reported for southern India, while they were smaller than those at the Satkhira
 392 station (7.58).

393 3.3 Processes Controlling $\delta^{18}O$ in Precipitation Over Bangladesh

394 3.3.1 Meteorological Elements Effects



395
 396 Figure 5: At the event scale, a strong and statistically significant negative correlation between
 397 $\delta^{18}O$ and relative humidity was observed at all three stations. The Sylhet and Satkhira stations
 398 revealed a significant association between $\delta^{18}O$ and air temperature; however, only the

399 Satkhira station reported a statistically significant association between precipitation amount
 400 and $\delta^{18}\text{O}$.

401 *Dansgaard* [1964] established the ‘temperature effect’ (decrease in δ -values with increasing
 402 temperature) and ‘amount effect’ (higher δ -values in sparse rain) as two of the important
 403 controls that influence variations in the isotopic compositions of precipitation. The
 404 temperature effect is significant in the temperate and polar regions while amount effect is
 405 primarily noticeable in low-latitude regions [*Zhang et al.*, 2019]. The majority of recent
 406 studies over the Indian subcontinent at different temporal resolutions ranging from event to
 407 interannual scales suggested that the amount effect is weak and even nonexistent in this
 408 region [*Araguas-Araguas et al.*, 1998; *Bhattacharya et al.*, 2003; *Breitenbach et al.*, 2010;
 409 *Datta et al.*, 1991; *Midhun et al.*, 2013; *Tang et al.*, 2015].

410 Table 3: Correlation coefficient between precipitation $\delta^{18}\text{O}$ and meteorological parameters

Station	$\delta^{18}\text{O}$ -RH	$\delta^{18}\text{O}$ -T	$\delta^{18}\text{O}$ -P
Barisal	-0.48**	-0.11	-0.15
Satkhira	-0.57**	0.30*	-0.32**
Sylhet	-0.23**	-0.43**	0.01

T = Temperature ($^{\circ}\text{C}$), P = Precipitation (mm), RH = Relative Humidity (%)

Numerals with ** and * represents statistically significant correlations at the 0.01 and 0.05 levels, respectively. Numerals without * indicates a failure to pass the significance test.

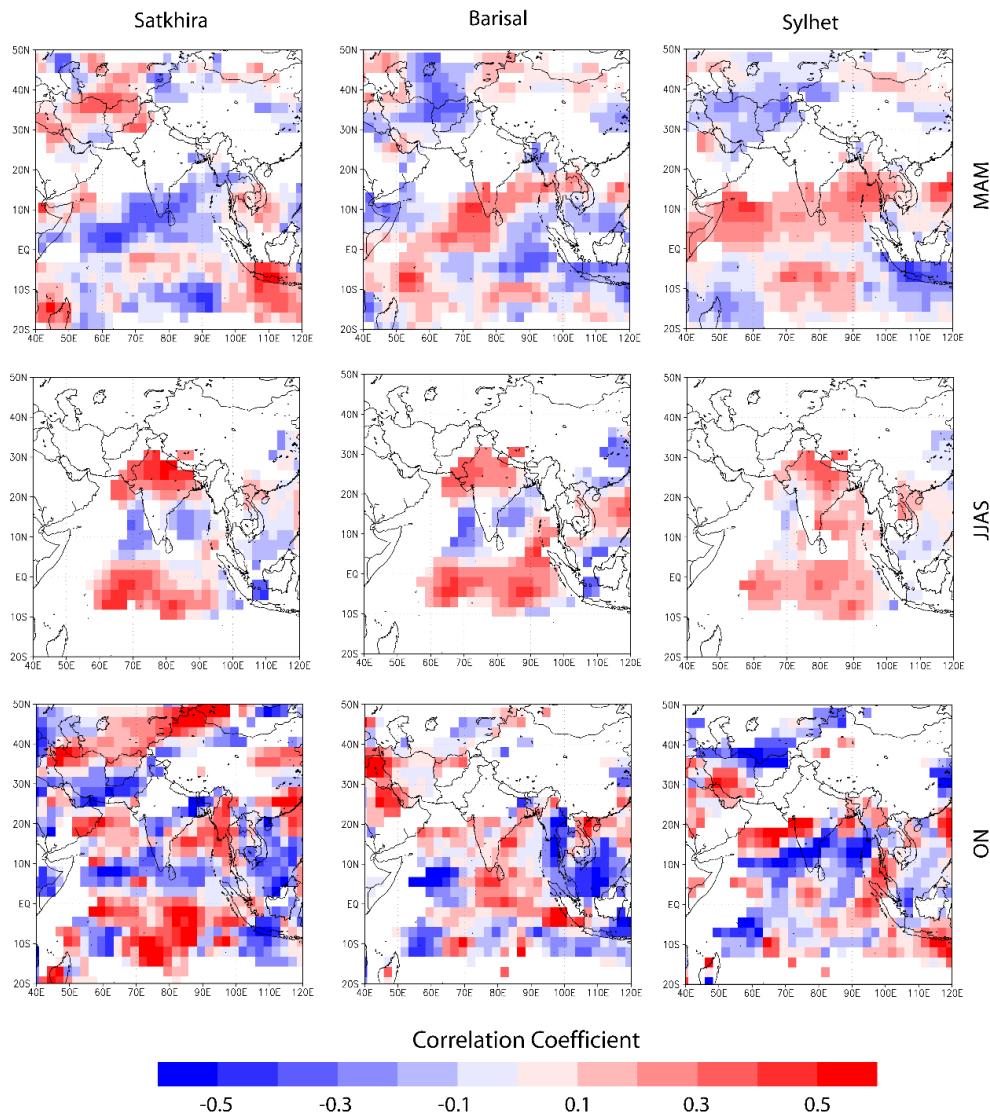
411 Here a weak ($n = 114$, $r = 0.30$) but statistically significant ($p < 0.01$) positive association
 412 between air temperature and $\delta^{18}\text{O}$ at Satkhira is found (Figure 5, Table 3). Such correlation
 413 gradually weakens from the west to east with a statistically significant negative relationship
 414 ($n = 258$, $r = -0.43$ $p < 0.01$) at Sylhet, however, it was weak and statistically insignificant at
 415 Barisal ($n = 130$, $r = -0.11$ $p > 0.05$). A statistically significant ($p < 0.01$) but moderately
 416 negative association between precipitation amount and event-based $\delta^{18}\text{O}$ at Satkhira ($n = 114$,
 417 $r = -0.32$) (Figure 6) was found; however, it was disappeared at Barisal ($n = 130$, $r = -0.15$)
 418 and Sylhet ($n = 258$, $r = 0.01$). *Tanoue et al.* [2018] and *Rahul and Ghosh* [2019] also
 419 reported an extremely weak ($r = -0.01$) relationship between $\delta^{18}\text{O}$ and precipitation amount in
 420 the region. All three stations revealed a significantly ($p < 0.01$) negative association between
 421 $\delta^{18}\text{O}$ and relative humidity and gradually decreases with increasing latitude or longitude from

422 southwest to northeast, with the strongest association at Satkhira (n = 114, r = -0.57) and the
423 weakest at Sylhet (n = 258, r = -0.23) as well as Barisal (n = 130, r = -0.48) in between.

424 Although we found statistically significant correlation between precipitation $\delta^{18}\text{O}$ and local
425 meteorological parameters (relative humidity, air temperature and precipitation amount), the
426 correlation between $\delta^{18}\text{O}$ and regional meteorological variation were statistically
427 insignificant. Correlation coefficients between the precipitation $\delta^{18}\text{O}$ measured at these three
428 stations and the precipitation amount/ temperature/humidity for the surrounding region are in
429 significant in all seasons. Thus, we suggest temperature, precipitation amount and humidity
430 are not dominant controls for event-based and seasonal variations of precipitation $\delta^{18}\text{O}$ at
431 Bangladesh.

432 **3.3.2 Influence of Convective Activities**

433 Convective activities impact precipitation events, which leave signals on stable isotopes in
434 precipitation, especially in tropical region [*Chakraborty et al.*, 2016; *Rahul et al.*, 2016;
435 *Saranya et al.*, 2018; *Wei et al.*, 2018]. OLR is widely considered to be a proxy for
436 convective activities. Low values indicate increase and intensive convective activities, vice
437 versa. To quantitatively account for the convective influence, we followed a simplified two-
438 step procedure. First, we quantified the deviation of OLR from the long-term average, which
439 allows us to formulate a simplified index of convective strength. Later, pixel-based
440 correlation coefficients were calculated to determine the regional OLR- $\delta^{18}\text{O}$ relationship at
441 the grid-point level, providing the estimation of the convective effects on $\delta^{18}\text{O}$. A significant
442 OLR increase (decrease) in a region with a negative (positive) OLR- $\delta^{18}\text{O}$ relationship can
443 justify the convective influence of $\delta^{18}\text{O}$ depletion (enrichment) in the region.



444

445 Figure 6: Spatial distribution of correlation coefficients between precipitation $\delta^{18}\text{O}$ and OLR
 446 indicating the relationship between convective activities in the region and $\delta^{18}\text{O}$ in different
 447 seasons during the 2017-2018 period. Correlation coefficients significant at $p < 0.05$ are
 448 displayed in the figure.

449 During MAM, the same convections result in the opposite variations of precipitation $\delta^{18}\text{O}$ in
 450 west and east Bangladesh, i.e. the strong convections above BOB associated with depleted
 451 $\delta^{18}\text{O}$ at Barisal and Sylhet, while enriched $\delta^{18}\text{O}$ at Satkhira (Figure 6). Similar influence was
 452 observed for Indonesia and stronger convective activities result in $\delta^{18}\text{O}$ enrichment at Barisal
 453 and Sylhet, while, Satkhira station experiences $\delta^{18}\text{O}$ depletion. Strong convective activities
 454 over Pakistan and Afghanistan also leads to $\delta^{18}\text{O}$ depletion (enrichment) at Satkhira (Barisal
 455 and Sylhet) stations. During JJAS, strong convective activities over IO, AS and north-western
 456 part of India leads to $\delta^{18}\text{O}$ depletion at all three stations. At Satkhira and Barisal stations

457 located to the south, strong convective activities over BoB resulted in $\delta^{18}\text{O}$ enrichment,
458 while, Sylhet station located to the north experienced $\delta^{18}\text{O}$ depletion. During ON, strong
459 convective activities over IO and BoB leads to $\delta^{18}\text{O}$ depletion (enrichment) at Barisal and
460 Satkhira (Sylhet) station. Convective activities over AS, however, leads to $\delta^{18}\text{O}$ enrichment at
461 all three stations. We did not have enough observations to perform statistical correlation
462 between $\delta^{18}\text{O}$ and OLR for DJF.

463 **3.4 Deuterium Excess and Moisture Source**

464 Many studies over the Tibetan Plateau have suggested that changes in the moisture source
465 region and moisture transport process significantly change the stable isotopes in precipitation
466 [Chen *et al.*, 2015; Li *et al.*, 2017; Li *et al.*, 2015; Meiliang *et al.*, 2014; Tang *et al.*, 2015;
467 Tian *et al.*, 2007; Wu *et al.*, 2015; Yu *et al.*, 2015; Yu *et al.*, 2014; Yu *et al.*, 2008]. Here, back
468 trajectory analysis with HYSPLIT for days with precipitation events revealed four main
469 moisture transport pathways for the stations, namely, southwest winds from the BoB,
470 southwest winds from the AS, southwest winds from the tropical IO, and continentally
471 recycled moisture (CR). Definitions for BoB, AS, IO and CR used in this study were
472 consistent with the classification system used by Tanoue *et al.* [2018]. Changes in specific
473 humidity along the clustered trajectories were also computed to obtain a clear visualization of
474 the moisture uptake process in the region.

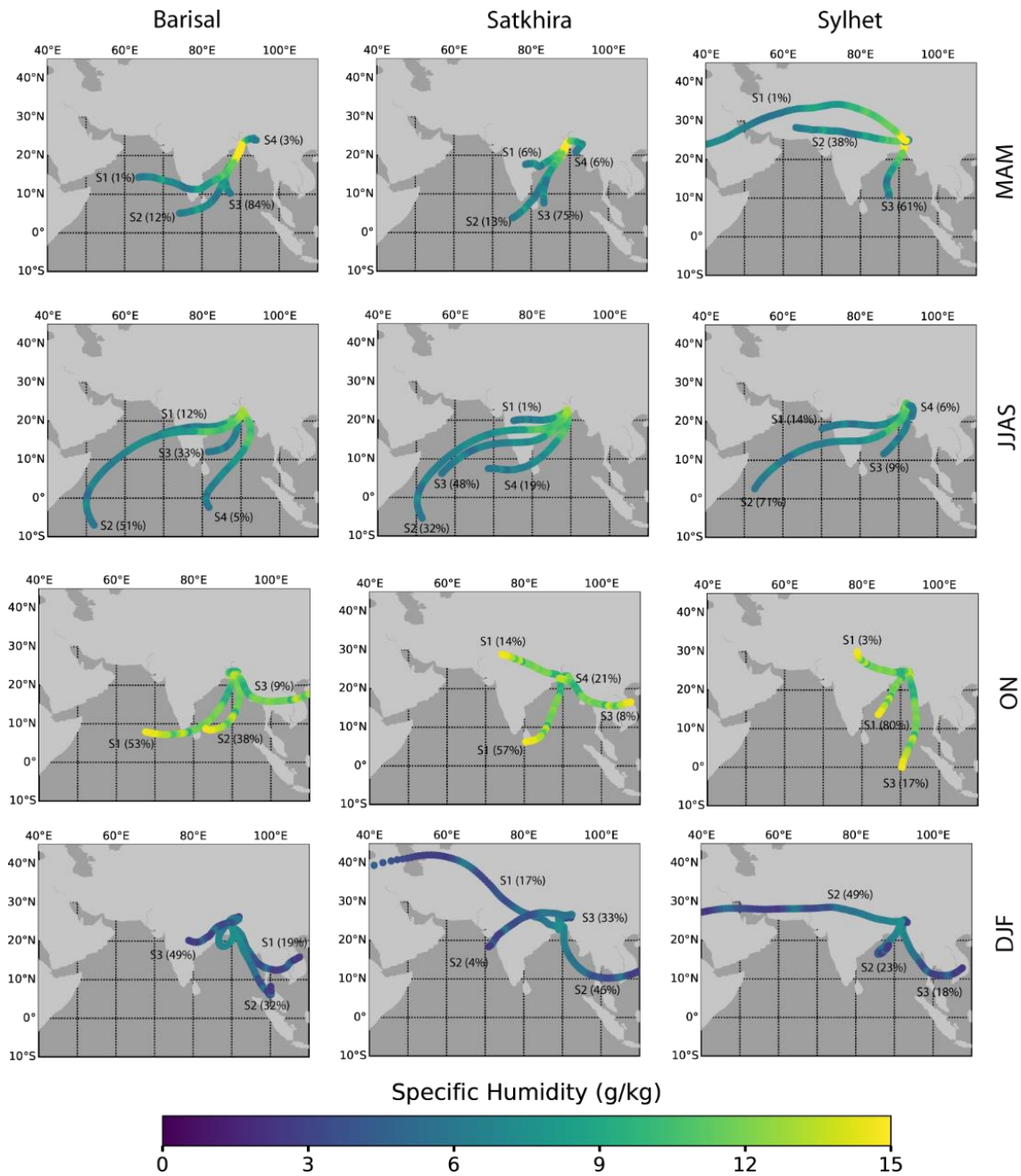
475 During MAM, moisture predominantly originated from the BoB and changes in specific
476 humidity along clustered trajectories were approximately 15.0 g/kg (Figure 7).
477 Approximately 64%, 51% and 56% of total airmass trajectories for Barisal, Satkhira and
478 Sylhet originated from the BoB. Neither Satkhira, nor Sylhet stations received any
479 contribution from AS where 1% of total trajectories for Barisal originated. Changes in
480 specific humidity along the clustered trajectories also indicated that the moisture uptake
481 process primarily occurred over the BoB suggesting greater influence of moisture from BoB
482 on stable isotopic variation in precipitation over Bangladesh. Tanoue *et al.* [2018] suggested
483 that, BoB and AS primarily contributed to MAM precipitation, however, we found very little
484 influence from AS with little moisture uptake, High amount-weighted $\delta^{18}\text{O}$ depletion (-
485 1.78‰) observed at the Barisal station could be associated with moisture from BoB that
486 accounted for 64% of total trajectories for the station. Primary moisture uptake over the BoB
487 through southerly winds contain highly depleted moisture [Bhattacharya *et al.*, 2003].

488 *Midhun et al.* [2018] confirmed that $\delta^{18}\text{O}$ -depleted precipitation events were associated with a
489 higher number of trajectories originating from the BoB. In our study, we found significant
490 influence of IO that accounted for 29%, 42% and 5% of total air mass trajectories for Barisal,
491 Satkhira and Sylhet stations, respectively. This indicated an eastward weakening of IO
492 influence with maximum (minimum) influence in western (eastern) part of Bangladesh.
493 Contributions from CR accounted for 5%, 7% and 39% of total air mass trajectories for
494 Barisal, Satkhira and Sylhet stations, respectively that brought moisture from India and
495 Mediterranean region. Higher amount-weighted $\delta^{18}\text{O}$ at the Satkhira station (0.88‰) with
496 very low deuterium excess (3.17‰) could be associated with BoB moisture that accounted
497 for >50% of total trajectories.

498 The $\delta^{18}\text{O}$ values started to decrease in the beginning of the monsoon season when a large
499 volume of moisture driven by the ISM started to move inland. During JJAS, moisture
500 transport from AS increased significantly (Figure 7). Contributions from AS accounted for
501 38%, 32% and 29% of total air mass trajectories for Barisal, Satkhira and Sylhet stations,
502 while, influence of BoB accounted for 9%, 8% and 9% of total trajectories for Barisal,
503 Satkhira and Sylhet stations. However, changes in specific humidity suggested that moisture
504 uptake primarily occurred over the BoB, with increase of specific humidity ~ 12.0 g/kg.
505 Continental moisture recycling supplied a large amount of the moisture originating over India
506 with increase of specific humidity ~ 10 g/kg, especially at Satkhira and Sylhet where 12% and
507 21% of total trajectories originated over land. The seasonal average $\delta^{18}\text{O}$ values were -
508 6.20‰, and -6.73‰ for Barisal and Sylhet, respectively, while they were significantly
509 enriched at Satkhira -4.22‰, due to the different moisture contribution between BOB and
510 CR. Both Sylhet and Satkhira stations received contributions from CR, however, only
511 Satkhira displayed isotopic enrichment because of the moisture origin. Moisture for Satkhira
512 originated from west-central part of India and arrived at Satkhira station located in the south-
513 western part of Bangladesh with relatively short air parcel travel distance. On the other hand,
514 moisture for Sylhet station originated at southern part of India and traveled long distance
515 before arriving at Sylhet station located at the north-eastern part of Bangladesh. *Breitenbach*
516 *et al.* [2010] demonstrated that longer travel distance resulted in $\delta^{18}\text{O}$ depletion, while,
517 shorter travel distance led to $\delta^{18}\text{O}$ enrichment over north-eastern part of India. Such
518 variations of moisture contributions through transport paths might have also resulted in
519 gradual increase of deuterium excess values from southwest to northeast (7.05‰ at Satkhira,
520 11.58‰ at the Barisal and 13.25‰ at Sylhet).

521 During ON, the BoB and AS supplied majority of the moisture that contributed to
522 precipitation in this season, and changes in specific humidity also suggested higher moisture
523 uptake along the BoB and AS branches of moisture transport. Contributions from the BoB
524 accounted for 38%, 34% and 25% of total trajectories for Barisal, Satkhira and Sylhet
525 stations. Sylhet station did not receive any contributions from AS, while, it accounted for
526 19% and 26% of total trajectories showing an eastward weakening of AS influence in the
527 season. CR accounted for 4%, 14% and 55% of total trajectories at Barisal, Satkhira and
528 Sylhet stations. Deuterium excess values at Barisal and Satkhira were 11.65‰ and 10.37‰,
529 while it was 12.06‰ at Sylhet station. Besides strong influence of CR that brought moisture
530 through westerly wind, 50% of total trajectories supplied locally recycled moisture that had
531 very short transport distance from the station that can explain increase in deuterium excess
532 values at Sylhet. Significant $\delta^{18}\text{O}$ depletion was recorded at Satkhira (-10.82‰) compared to
533 that of Barisal (-8.99‰) and Sylhet (-8.89‰). Such a $\delta^{18}\text{O}$ depletion at Satkhira might have
534 occurred due to heavy rainfall events of October 20-22, 2017 when $\delta^{18}\text{O}$ values at Satkhira
535 became as low as -20.0‰.

536 During DJF, BoB accounted for 32%, 4% and 23% of total trajectories for Barisal, Satkhira
537 and Sylhet stations. AS accounted for 4% of total trajectories for Satkhira, however, Barisal
538 and Sylhet did not receive any contributions from AS. CR accounted for 69%, 75% and 72%
539 of total trajectories for Barisal, Satkhira and Sylhet. IO accounted for 5% of total trajectories
540 for Satkhira. Satkhira station did not have any precipitation samples for DJF and the number
541 of samples for Sylhet and Barisal were small making our confidence limited for isotopic
542 variation in the season. Average amount weighted $\delta^{18}\text{O}$ for Barisal and Sylhet were -7.79‰
543 and -5.81‰, while, it was 12.70‰ and 13.71‰ for deuterium excess, respectively. Higher
544 deuterium excess value for Sylhet might have resulted from stronger (59% of total
545 trajectories) influence of westerly wind that brought moisture from the Mediterranean region
546 and north-western part of India.



547

548 Figure 7: Specific humidity plotted along the clustered trajectory showing the moisture
 549 uptake process in the region

550 *Tanoue et al.* [2018] suggested that moisture from BoB and AS primarily contributed to
 551 MAM precipitation, however, we found little influence of AS in MAM at all three stations.
 552 Satkhira and Sylhet station did not receive any contribution, while, only 1% of total
 553 trajectories originated over AS. According to *Tanoue et al.* [2018], the influence from BoB
 554 and AS decreased significantly in JJAS and moisture predominantly originated from IO.
 555 However, our study found ~30% of total airmass trajectories at all three stations originating

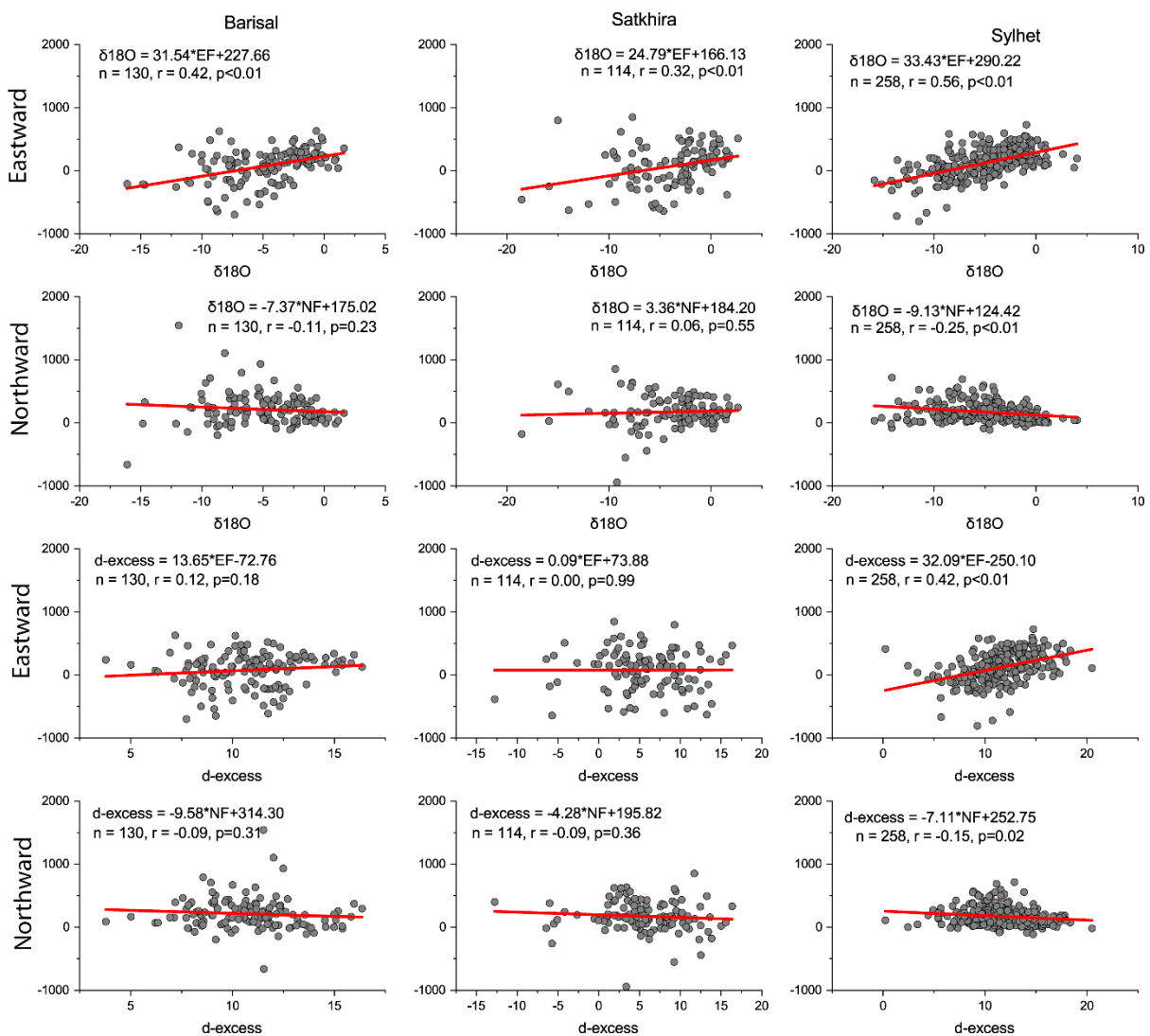
556 over AS, while, maximum moisture uptake process occurred over BoB that accounted for
557 ~8% of total trajectories. Indeed, ~50% of total trajectories originated over IO, however,
558 moisture uptake over IO were very small. *Tanoue et al.* [2018] reported origin for ~30% of
559 total trajectories as PO, however, we found ~8% of total trajectories that originated over PO.
560 Although we found similar percentage of trajectories originating from the BoB at Sylhet
561 station, it was significantly different for CR that revealed significantly higher percentages
562 (55%) than that being reported (37%) previously [*Tanoue et al.*, 2018].

563

564 Except a significant depletion at Satkhira, monthly amount weighted deuterium excess values
565 lacked any regular pattern. Only Sylhet station revealed a regular maximum value in May
566 (~13.5‰), while, minimum values occurred in July (2017) and September (2018). At Sylhet,
567 minimum value was ~8.5‰, while, it was extremely depleted at Satkhira (0.09‰) that
568 occurred in June 2017. As Satkhira, we found maximum values in June 2018 (11.11‰),
569 however, June 2017 had very depleted (2.91‰) values. Throughout the study period,
570 deuterium excess values remained within the 0.09‰ to 15.0‰ range at these three stations.
571 Deuterium excess values showed a consistent eastward increasing trend with lowest values at
572 Satkhira and highest values at Sylhet in MAM, JJAS and ON. Satkhira station did not have
573 any observation for DJF and we found highest deuterium excess values at Barisal.

574 To quantitatively account for the moisture source influence, we investigated vapor flux
575 anomalies and examined their influence on $\delta^{18}\text{O}$. In the 2017 MAM, northward flux
576 anomalies were positive within the 20°S and 20°N latitudes. Within the 20°N and 40°N
577 latitudes, the northward flux had slightly lower values (~5 kg/m/s) than the long-term average
578 (Figure S1). In the 2018 MAM, a significant decrease in the northward flux was experienced
579 within the equator and 30°N latitude, with the lowest values at 15°N, where the northward
580 flux was ~18 kg/m/s. On the other hand, little variation in the eastward flux anomalies was
581 observed in 2017 and remained closely aligned with the long-term average; however, a
582 significant decrease in the eastward flux anomalies was found for 2018 within the 60°E and
583 130°E longitudes. Although the difference between the 2017 and 2018 northward flux
584 anomalies over the BGD_Domain (rectangular region in between latitude 20°N-26°N and
585 longitude 88°E-92°E) was minute, it was significantly higher (as high as ~60 kg/m/s at 90°E)
586 for the eastward vapor flux. In JJAS of both 2017 and 2018, the northward flux anomalies
587 were significantly higher (~20 kg/m/s) than the long-term averages within the 20°S and 15°N

588 latitudes; however, differences between 2017 and 2018 were significantly higher within the
 589 15°N and 30°N latitudes. The 2018 anomalies were closely aligned with the long-term
 590 average, while it was 25 kg/m/s higher in 2017. Although the eastward flux revealed similar
 591 variations, we found large differences in anomalies for 2018 within the 70°E and 130°E
 592 longitudes. Both eastward and northward fluxes showed large differences between 2017 and
 593 2018 over the BGD_Domain. In ON, northward flux anomalies remained similar in 2017 and
 594 2018, with values closely aligned with the long-term average. However, large differences in
 595 the eastward flux anomalies were found over the 60°E and 110°E longitudes, where the
 596 difference between the 2017 and 2018 anomalies was ~40 kg/m/s.



597

598 Figure 8: Influence of eastward and northward vapor fluxes on precipitation $\delta^{18}O$ and
 599 deuterium excess.

600 To investigate the influence of moisture flux on precipitation stable isotopic variation over
601 Bangladesh, correlations between precipitation $\delta^{18}\text{O}$ and moisture flux are calculated at three
602 stations. Based on vapor flux data from the ERA5 reanalysis, The zonal average of the
603 northward (between 40°E and 130°E longitude) and eastward (between 20°S and 40°N
604 latitude) vapor flux anomalies displayed significant variation within the BGD_Domain.
605 relationships between the $\delta^{18}\text{O}$ and eastward fluxes were intensifying from southwest to
606 northeast ($p < 0.01$), showing the strongest at Sylhet ($n = 258$, $r = 0.56$) and the weakest at
607 Satkhira ($n = 114$, $r = 0.32$), which is not consistent with the finding on the Eastern Tibetan
608 Plateau [Tian *et al.* [2008]]. weak and insignificant relationships between the $\delta^{18}\text{O}$ and
609 northward fluxes at Satkhira ($n = 114$, $r = 0.06$) and Barisal ($n = 130$, $r = -0.11$) were found,
610 while the relationship was significantly moderate ($p < 0.01$) at the Sylhet ($n = 258$, $r = -0.25$)
611 (Figure 8). Deuterium excess at Barisal and Satkhira displayed a weak relationship with both
612 the eastward and northward vapor fluxes; however, this relationship was statistically
613 significant at the Sylhet station. At Sylhet, the relationship between the eastward flux and
614 deuterium excess ($r = 0.42$, $p < 0.01$) was stronger than the relationship between the northward
615 vapor flux and deuterium excess ($r = -0.15$, $p < 0.05$), which is consistent with back
616 trajectories and OLR analysis in above sections.

617 **4. Conclusions**

618 We investigated the local and regional controls of the seasonal variations in precipitation
619 $\delta^{18}\text{O}$ over Bangladesh, based on an event-based precipitation sample analysis during the
620 2017-2018 period. Precipitation $\delta^{18}\text{O}$ displayed a distinct temporal and spatial pattern having
621 the highest values in March following gradual decrease until it became the lowest in October.
622 Amount weighted $\delta^{18}\text{O}$ values displayed a decreasing trend with increasing latitude which is
623 consistent with current understanding on spatial variation in precipitation stable isotopes over
624 India and Tibetan Plateau where monsoon dominates the moisture transport. In DJF, $\delta^{18}\text{O}$ and
625 δD displayed the most enriched values at the northern station (Sylhet), while, it was
626 significantly depleted at Barisal station located in the south. $\delta^{18}\text{O}$ and δD displayed eastward
627 depletion in MAM and JJAS with most enriched (depleted) values over the western (eastern)
628 part of Bangladesh. We found the most depleted deuterium excess values over the western
629 part of Bangladesh, while, it was the most enriched at the station to the east. $\delta^{18}\text{O}$ and δD
630 values for ON displayed the opposite pattern of MAM and JJAS and we found the most
631 enriched $\delta^{18}\text{O}$ and δD values over the eastern part of Bangladesh.

632 We performed a comparison between the response of MAM and ON heavy rainfall events on
633 stable isotopic composition of precipitation and it was found that, MAM heavy rainfall events
634 do not cause significant isotopic depletion that is typical of JJAS and ON heavy rainfall
635 events. By performing back trajectory analysis, we found that moisture source was different
636 for these two types of heavy rainfall events. MAM heavy rainfall events received moisture
637 through continental recycling, while, ON events received moisture from IO, BoB and AS.

638 We report the existence of a strong convective effect that influence stable isotopic variation
639 in precipitation over Bangladesh. Strong convective activities over BoB, AS and IO
640 significantly influence stable isotopic composition throughout the year. We also
641 demonstrated a significant influence of moisture source region and flux on $\delta^{18}\text{O}$ variation.
642 Our study suggests that, Eastward vapor flux displayed statistically significant correlation
643 with both $\delta^{18}\text{O}$ and deuterium excess which is inconsistent with the results obtained over the
644 Tibetan Plateau. The shifts of moisture contribution from BoB, AS and IO primarily
645 influence stable isotopic composition in precipitation, especially in JJAS and ON. Changes in
646 specific humidity along the trajectory revealed that, despite having larger percentages of
647 airmass trajectories originates over IO or AS, BoB still controls variations of precipitation
648 stable isotopes over the Bangladesh because of a larger share of moisture uptake.

649 **Acknowledgements.**

650 This work is jointly supported by Strategic Priority Research Program of Chinese Academy
651 of Sciences (Grant No. 2019QZKK0208) and National Natural Science Foundation of China
652 (Grant No. 41922002 and 41871068). We acknowledge anonymous reviewers, whose
653 comments and suggestions greatly improved the manuscript. We would also like to thank all
654 the staff members of the Bangladesh Atomic Energy Commission (BAEC) who contributed
655 to collection and storage of precipitation samples. Authors would like to thank Di Dai and Dr.
656 Dongmei Qu for their cooperation during laboratory analysis. ECMWF ERA5 reanalysis
657 datasets used in this study were retrieved from cds.climate.copernicus.eu/. TRMM datasets
658 can be accessed from <https://disc.gsfc.nasa.gov/>.

659

660 **References**

661 Ahmed, R., and S. Karmakar (1993), Arrival and Withdrawal Dates of the Summer Monsoon in
662 Bangladesh, *International Journal of Climatology*, 13(7), 727-740, doi:10.1002/joc.3370130703.

663 Ananthkrishnan, R., and M. K. Soman (1988), The Onset of the Southwest Monsoon over Kerala -
664 1901-1980, *Journal of Climatology*, 8(3), 283-296, doi:10.1002/joc.3370080305.

665 Araguas-Araguas, L., K. Froehlich, and K. Rozanski (1998), Stable isotope composition of precipitation
666 over southeast Asia, *Journal of Geophysical Research-Atmospheres*, 103(D22), 28721-28742,
667 doi:10.1029/98jd02582.

668 Bershaw, J. (2018), Controls on Deuterium Excess across Asia, *Geosciences*, 8(7), 257,
669 doi:10.3390/geosciences8070257.

670 Bhattacharya, S. K., K. Froehlich, P. K. Aggarwal, and K. M. Kulkarni (2003), Isotopic variation in
671 Indian Monsoon precipitation: Records from Bombay and New Delhi, *Geophysical Research Letters*,
672 30(24), doi:10.1029/2003gl018453.

673 Breitenbach, S. F. M., J. F. Adkins, H. Meyer, N. Marwan, K. K. Kumar, and G. H. Haug (2010), Strong
674 influence of water vapor source dynamics on stable isotopes in precipitation observed in Southern
675 Meghalaya, NE India, *Earth and Planetary Science Letters*, 292(1-2), 212-220,
676 doi:10.1016/j.epsl.2010.01.038.

677 Cai, Z. Y., and L. D. Tian (2016), Atmospheric Controls on Seasonal and Interannual Variations in the
678 Precipitation Isotope in the East Asian Monsoon Region, *Journal of Climate*, 29(4), 1339-1352,
679 doi:10.1175/Jcli-D-15-0363.1.

680 Cai, Z. Y., L. D. Tian, and G. J. Bowen (2018), Spatial-seasonal patterns reveal large-scale atmospheric
681 controls on Asian Monsoon precipitation water isotope ratios, *Earth and Planetary Science Letters*,
682 503, 158-169, doi:10.1016/j.epsl.2018.09.028.

683 Chakraborty, S., N. Sinha, R. Chattopadhyay, S. Sengupta, P. M. Mohan, and A. Datye (2016),
684 Atmospheric controls on the precipitation isotopes over the Andaman Islands, Bay of Bengal,
685 *Scientific Reports*, 6, 19555, doi:10.1038/srep19555.

686 Chen, F. L., M. J. Zhang, Q. Ma, S. J. Wang, X. F. Li, and X. F. Zhu (2015), Stable isotopic characteristics
687 of precipitation in Lanzhou City and its surrounding areas, Northwest China, *Environmental Earth*
688 *Sciences*, 73(8), 4671-4680, doi:10.1007/s12665-014-3776-6.

689 Craig, H. (1961), Isotopic Variations in Meteoric Waters, *Science*, 133(3465), 1702-1703,
690 doi:10.1126/science.133.3465.1702.

691 Crawford, J., C. E. Hughes, and S. Lykoudis (2014), Alternative least squares methods for determining
692 the meteoric water line, demonstrated using GNIP data, *Journal of Hydrology*, 519, 2331-2340,
693 doi:10.1016/j.jhydrol.2014.10.033.

694 Dansgaard, W. (1964), Stable Isotopes in Precipitation, *Tellus*, 16(4), 436-468, doi:10.1111/j.2153-
695 3490.1964.tb00181.x.

696 Das, S. (2017), Performance of region-of-influence approach of frequency analysis of extreme rainfall
697 in monsoon climate conditions, *International Journal of Climatology*, 37(S1), 612-623,
698 doi:10.1002/joc.5025.

699 Datta, P. S., S. K. Tyagi, and H. Chandrasekharan (1991), Factors Controlling Stable Isotope
700 Composition of Rainfall in New-Delhi, India, *Journal of Hydrology*, 128(1-4), 223-236,
701 doi:10.1016/0022-1694(91)90139-9.

702 Day, J. A., I. Fung, and C. Risi (2015), Coupling of South and East Asian Monsoon Precipitation in July-
703 August*, *Journal of Climate*, 28(11), 4330-4356, doi:10.1175/Jcli-D-14-00393.1.

704 Dewan, A., E. T. Ongee, M. Rafiuddin, M. M. Rahman, and R. Mahmood (2018), Lightning activity
705 associated with precipitation and CAPE over Bangladesh, *International Journal of Climatology*, 38(4),
706 1649-1660, doi:10.1002/joc.5286.

707 Fahad, M. G. R., A. K. M. S. Islam, R. Nazari, M. A. Hasan, G. M. T. Islam, and S. K. Bala (2018),
708 Regional changes of precipitation and temperature over Bangladesh using bias-corrected multi-

709 model ensemble projections considering high-emission pathways, *International Journal of*
710 *Climatology*, 38(4), 1634-1648, doi:10.1002/joc.5284.

711 Hughes, C. E., and J. Crawford (2012), A new precipitation weighted method for determining the
712 meteoric water line for hydrological applications demonstrated using Australian and global GNIP
713 data, *Journal of Hydrology*, 464, 344-351, doi:10.1016/j.jhydrol.2012.07.029.

714 Jeelani, G., R. D. Deshpande, M. Galkowski, and K. Rozanski (2018), Isotopic composition of daily
715 precipitation along the southern foothills of the Himalayas: impact of marine and continental
716 sources of atmospheric moisture, *Atmospheric Chemistry and Physics*, 18(12), 8789-8805,
717 doi:10.5194/acp-18-8789-2018.

718 Kostrova, S. S., H. Meyer, F. Fernandez, M. Werner, and P. E. Tarasov (2020), Moisture origin and
719 stable isotope characteristics of precipitation in southeast Siberia, *Hydrological Processes*, 34(1), 51-
720 67, doi:10.1002/hyp.13571.

721 Kumar, B., S. P. Rai, U. S. Kumar, S. K. Verma, P. Garg, S. V. V. Kumar, R. Jaiswal, B. K. Purendra, S. R.
722 Kumar, and N. G. Pande (2010), Isotopic characteristics of Indian precipitation, *Water Resources*
723 *Research*, 46, doi:10.1029/2009wr008532.

724 Lekshmy, P. R., M. Midhun, and R. Ramesh (2015), Spatial variation of amount effect over peninsular
725 India and Sri Lanka: Role of seasonality, *Geophysical Research Letters*, 42(13), 5500-5507,
726 doi:10.1002/2015gl064517.

727 Li, G., X. P. Zhang, Y. P. Xu, Y. F. Wang, and H. W. Wu (2017), Synoptic time-series surveys of
728 precipitation delta O-18 and its relationship with moisture sources in Yunnan, southwest China,
729 *Quaternary International*, 440, 40-51, doi:10.1016/j.quaint.2016.03.014.

730 Li, J., T. Tao, Z. H. Pang, M. Tan, Y. L. Kong, W. H. Duan, and Y. W. Zhang (2015), Identification of
731 Different Moisture Sources through Isotopic Monitoring during a Storm Event, *Journal of*
732 *Hydrometeorology*, 16(4), 1918-1927, doi:10.1175/Jhm-D-15-0005.1.

733 Meiliang, Z., Z. Xiaoyan, W. Xia, Y. Jianjun, and P. Moucheng (2014), $\delta^{18}\text{O}$ characteristics of meteoric
734 precipitation and its water vapor sources in the Guilin area of China, *Environmental Earth Sciences*,
735 74(2), 953-976, doi:10.1007/s12665-014-3827-z.

736 Midhun, M., P. R. Lekshmy, and R. Ramesh (2013), Hydrogen and oxygen isotopic compositions of
737 water vapor over the Bay of Bengal during monsoon, *Geophysical Research Letters*, 40(23), 6324-
738 6328, doi:10.1002/2013gl058181.

739 Midhun, M., P. R. Lekshmy, R. Ramesh, K. Yoshimura, K. K. Sandeep, S. Kumar, R. Sinha, A. Singh, and
740 S. Srivastava (2018), The Effect of Monsoon Circulation on the Stable Isotopic Composition of
741 Rainfall, *Journal of Geophysical Research-Atmospheres*, 123(10), 5205-5221,
742 doi:10.1029/2017jd027427.

743 Mukherjee, A., A. E. Fryar, and H. D. Rowe (2007), Regional-scale stable isotopic signatures of
744 recharge and deep groundwater in the arsenic affected areas of West Bengal, India, *Journal of*
745 *Hydrology*, 334(1-2), 151-161, doi:10.1016/j.jhydrol.2006.10.004.

746 Mullick, M. R. A., R. M. Nur, M. J. Alam, and K. M. A. Islam (2019), Observed trends in temperature
747 and rainfall in Bangladesh using pre-whitening approach, *Global and Planetary Change*, 172, 104-
748 113, doi:10.1016/j.gloplacha.2018.10.001.

749 Munksgaard, N. C., C. Zwart, J. Haig, L. A. Cernusak, and M. I. Bird (2020), Coupled rainfall and water
750 vapour stable isotope time series reveal tropical atmospheric processes on multiple timescales,
751 *Hydrological Processes*, 34(1), 111-124, doi:10.1002/hyp.13576.

752 Pour, S. H., S. Shahid, E. S. Chung, and X. J. Wang (2018), Model output statistics downscaling using
753 support vector machine for the projection of spatial and temporal changes in rainfall of Bangladesh,
754 *Atmospheric Research*, 213, 149-162, doi:10.1016/j.atmosres.2018.06.006.

755 Putman, A. L., R. P. Fiorella, G. J. Bowen, and Z. Y. Cai (2019), A Global Perspective on Local Meteoric
756 Water Lines: Meta-analytic Insight Into Fundamental Controls and Practical Constraints, *Water*
757 *Resources Research*, 55(8), 6896-6910, doi:10.1029/2019wr025181.

758 Rafiuddin, M., H. Uyeda, and M. N. Islam (2010), Characteristics of monsoon precipitation systems in
759 and around Bangladesh, *International Journal of Climatology*, 30(7), 1042-1055,
760 doi:10.1002/joc.1949.

761 Rahul, P., and P. Ghosh (2019), Long term observations on stable isotope ratios in rainwater samples
762 from twin stations over Southern India; identifying the role of amount effect, moisture source and
763 rainout during the dual monsoons, *Climate Dynamics*, 52(11), 6893-6907, doi:10.1007/s00382-018-
764 4552-1.

765 Rahul, P., P. Ghosh, S. K. Bhattacharya, and K. Yoshimura (2016), Controlling factors of rainwater and
766 water vapor isotopes at Bangalore, India: Constraints from observations in 2013 Indian monsoon,
767 *Journal of Geophysical Research-Atmospheres*, 121(23), 13936-13952, doi:10.1002/2016jd025352.

768 Rimi, R. H., K. Haustein, M. R. Allen, and E. J. Barbour (2019), Risks of Pre-Monsoon Extreme Rainfall
769 Events of Bangladesh: Is Anthropogenic Climate Change Playing a Role?, *Bulletin of the American*
770 *Meteorological Society*, 100(1), S61-S65, doi:10.1175/bams-d-18-0152.1.

771 Rohrmann, A., M. R. Strecker, B. Bookhagen, A. Mulch, D. Sachse, H. Pingel, R. N. Alonso, T. F.
772 Schildgen, and C. Montero (2014), Can stable isotopes ride out the storms? The role of convection
773 for water isotopes in models, records, and paleoaltimetry studies in the central Andes, *Earth and*
774 *Planetary Science Letters*, 407, 187-195, doi:10.1016/j.epsl.2014.09.021.

775 Saranya, P., G. Krishan, M. S. Rao, S. Kumar, and B. Kumar (2018), Controls on water vapor isotopes
776 over Roorkee, India: Impact of convective activities and depression systems, *Journal of Hydrology*,
777 557, 679-687, doi:10.1016/j.jhydrol.2017.12.061.

778 Sinha, N., and S. Chakraborty (2020), Isotopic interaction and source moisture control on the isotopic
779 composition of rainfall over the Bay of Bengal, *Atmospheric Research*, 235, 104760,
780 doi:10.1016/j.atmosres.2019.104760.

781 Sinha, N., S. Chakraborty, R. Chattopadhyay, B. N. Goswami, P. M. Mohan, D. K. Parua, D. Sarma, A.
782 Datye, S. Sengupta, S. Bera, and K. K. Baruah (2019), Isotopic investigation of the moisture transport
783 processes over the Bay of Bengal, *Journal of Hydrology X*, 2, 100021,
784 doi:10.1016/j.hydroa.2019.100021.

785 Stein, A. F., R. R. Draxler, G. D. Rolph, B. J. B. Stunder, M. D. Cohen, and F. Ngan (2015), NOAA's
786 Hysplit Atmospheric Transport and Dispersion Modeling System, *Bulletin of the American*
787 *Meteorological Society*, 96(12), 2059-2077, doi:10.1175/BAMS-D-14-00110.1.

788 Tang, Y., H. Pang, W. Zhang, Y. Li, S. Wu, and S. Hou (2015), Effects of changes in moisture source
789 and the upstream rainout on stable isotopes in precipitation - a case study in Nanjing, eastern China,
790 *Hydrology and Earth System Sciences*, 19(10), 4293-4306, doi:10.5194/hess-19-4293-2015.

791 Tanoue, M., K. Ichiyonagi, K. Yoshimura, M. Kiguchi, T. Terao, and T. Hayashi (2018), Seasonal
792 variation in isotopic composition and the origin of precipitation over Bangladesh, *Progress in Earth*
793 *and Planetary Science*, 5(1), 77, doi:10.1186/s40645-018-0231-4.

794 Tian, L. D., L. L. Ma, W. S. Yu, Z. F. Liu, C. L. Yin, Z. P. Zhao, W. Tang, and Y. Wang (2008), Seasonal
795 variations of stable isotope in precipitation and moisture transport at Yushu, eastern Tibetan
796 Plateau, *Science in China Series D-Earth Sciences*, 51(8), 1121-1128, doi:10.1007/s11430-008-0089-1.

797 Tian, L. D., T. D. Yao, K. MacClune, J. W. C. White, A. Schilla, B. Vaughn, R. Vachon, and K. Ichiyonagi
798 (2007), Stable isotopic variations in west China: A consideration of moisture sources, *Journal of*
799 *Geophysical Research-Atmospheres*, 112(D10), doi:10.1029/2006jd007718.

800 Vimeux, F., R. Gallaire, S. Bony, G. Hoffmann, and J. Chiang (2005), What are the climate controls on
801 δD in precipitation in the Zongo Valley (Bolivia)? Implications for the Illimani ice core interpretation,
802 *Earth and Planetary Science Letters*, 240(2), 205-220, doi:10.1016/j.epsl.2005.09.031.

803 Wang, L. H., Y. H. Dong, D. M. Han, and Z. F. Xu (2019), Stable isotopic compositions in precipitation
804 over wet island in Central Asia, *Journal of Hydrology*, 573, 581-591,
805 doi:10.1016/j.jhydrol.2019.04.005.

806 Wei, Z. W., X. Lee, Z. F. Liu, U. Seeboonruang, M. Koike, and K. Yoshimura (2018), Influences of large-
807 scale convection and moisture source on monthly precipitation isotope ratios observed in Thailand,
808 Southeast Asia, *Earth and Planetary Science Letters*, 488, 181-192, doi:10.1016/j.epsl.2018.02.015.

809 Whitehead, P., G. Bussi, M. A. Hossain, M. Dolk, P. Das, S. Comber, R. Peters, K. J. Charles, R. Hope,
810 and M. S. Hossain (2018), Restoring water quality in the polluted Turag-Tongi-Balu river system,
811 Dhaka: Modelling nutrient and total coliform intervention strategies, *Science of the Total*
812 *Environment*, 631-632, 223-232, doi:10.1016/j.scitotenv.2018.03.038.

813 Wu, H. W., X. Y. Li, J. M. Zhang, J. Li, J. Z. Liu, L. H. Tian, and C. Fu (2019), Stable isotopes of
814 atmospheric water vapour and precipitation in the northeast Qinghai-Tibetan Plateau, *Hydrological*
815 *Processes*, 33(23), 2997-3009, doi:10.1002/hyp.13541.

816 Wu, H. W., X. P. Zhang, X. Y. Li, G. Li, and Y. M. Huang (2015), Seasonal variations of deuterium and
817 oxygen-18 isotopes and their response to moisture source for precipitation events in the subtropical
818 monsoon region, *Hydrological Processes*, 29(1), 90-102, doi:10.1002/hyp.10132.

819 Yang, H., K. R. Johnson, M. L. Griffiths, and K. Yoshimura (2016), Interannual controls on oxygen
820 isotope variability in Asian monsoon precipitation and implications for paleoclimate reconstructions,
821 *Journal of Geophysical Research-Atmospheres*, 121(14), 8410-8428, doi:10.1002/2015jd024683.

822 Yao, T., V. Masson-Delmotte, J. Gao, W. Yu, X. Yang, C. Risi, C. Sturm, M. Werner, H. Zhao, Y. He, W.
823 Ren, L. Tian, C. Shi, and S. Hou (2013), A review of climatic controls on $\delta^{18}\text{O}$ in precipitation over the
824 Tibetan Plateau: Observations and simulations, *Reviews of Geophysics*, 51(4), 525-548,
825 doi:10.1002/rog.20023.

826 Yu, W., L. Tian, Y. Ma, B. Xu, and D. Qu (2015), Simultaneous monitoring of stable oxygen isotope
827 composition in water vapour and precipitation over the central Tibetan Plateau, *Atmospheric*
828 *Chemistry and Physics*, 15(18), 10251-10262, doi:10.5194/acp-15-10251-2015.

829 Yu, W. S., T. D. Yao, S. Lewis, L. D. Tian, Y. M. Ma, B. Q. Xu, and D. M. Qu (2014), Stable oxygen
830 isotope differences between the areas to the north and south of Qinling Mountains in China reveal
831 different moisture sources, *International Journal of Climatology*, 34(6), 1760-1772,
832 doi:10.1002/joc.3799.

833 Yu, W. S., T. D. Yao, L. Tian, Y. M. Ma, K. P. Ichlyanagi, Y. Wang, and W. Z. Sun (2008), Relationships
834 between delta O-18 in precipitation and air temperature and moisture origin on a south-north
835 transect of the Tibetan Plateau, *Atmospheric Research*, 87(2), 158-169,
836 doi:10.1016/j.atmosres.2007.08.004.

837 Zhang, T., Y. S. Zhang, Y. H. Gun, N. Ma, D. Dai, H. T. Song, D. M. Qu, and H. F. Gao (2019), Controls of
838 stable isotopes in precipitation on the central Tibetan Plateau: A seasonal perspective, *Quaternary*
839 *International*, 513, 66-79, doi:10.1016/j.quaint.2019.03.031.

840

841